Diffusion of curcumin in PLGA-based carriers for drug delivery: a molecular dynamics study

Journal of Molecular Modeling (2024) 30:219
https://doi.org/10.1007/s00894-024-06023-x

ORIGINAL PAPER

Diffusion of curcumin in PLGA-based carriers for drug delivery: a molecular dynamics study

Alessandro De Giorgi[1] · Francesco Maria Bellussi[1] · Stefano Parlani[1] · Andrea Lucisano[1] · Emanuele Silvestri[1] · Susmita Aryal[2] · Sanghyo Park[2] · Jaehong Key[2] · Matteo Fasano[1]

Received: 19 February 2024 / Accepted: 11 June 2024

Abstract

Context: The rapid growth and diversification of drug delivery systems have been significantly supported by advancements in micro- and nano-technologies, alongside the adoption of biodegradable polymeric materials like poly(lactic-co-glycolic acid) (PLGA) as microcarriers. These developments aim to reduce toxicity and enhance target specificity in drug delivery. The use of *in silico* methods, particularly molecular dynamics (MD) simulations, has emerged as a pivotal tool for predicting the dynamics of species within these systems. This approach aids in investigating drug delivery mechanisms, thereby reducing the costs associated with design and prototyping. In this study, we focus on elucidating the diffusion mechanisms in curcumin-loaded PLGA particles, which are critical for optimizing drug release and efficacy in therapeutic applications.

Methods: We utilized MD to explore the diffusion behavior of curcumin in PLGA drug delivery systems. The simulations, executed with GROMACS, modeled curcumin molecules in a representative volume element of PLGA chains and water, referencing molecular structures from the Protein Data Bank and employing the CHARMM force field. We generated PLGA chains of varying lengths using the Polymer Modeler tool and arranged them in a bulk-like environment with Packmol. The simulation protocol included steps for energy minimization, T and p equilibration, and calculation of the isotropic diffusion coefficient from the mean square displacement. The Taguchi method was applied to assess the effects of hydration level, PLGA chain length, and density on diffusion.

Results: Our results provide insight into the influence of PLGA chain length, hydration level, and polymer density on the diffusion coefficient of curcumin, offering a mechanistic understanding for the design of efficient drug delivery systems. The sensitivity analysis obtained through the Taguchi method identified hydration level and PLGA density as the most significant input parameters affecting curcumin diffusion, while the effect of PLGA chain length was negligible within the simulated range. We provided a regression equation capable to accurately fit MD results. The regression equation suggests that increases in hydration level and PLGA density result in a decrease in the diffusion coefficient.

Keywords Diffusion · Polymeric carriers · Molecular dynamics · Water · Mass transfer

Introduction

Curcumin, a yellow crystalline powder, is a polyphenolic compound extracted from the rhizome of the Curcuma longa [1]. Over the past years, it has drawn attention due to its diverse pharmacological activities like anti-carcinogenic, anti-inflammatory, antioxidant, antibacterial, and anti-proliferative [2–4]. However, the clinical use of curcumin is still limited due to its low solubility, low bioavailability, rapid metabolism, lower gastrointestinal absorption, and low permeability, which limit the therapeutic success of curcumin [5, 6]. In the quest to overcome the bioavailability issues and enhance its properties, better drug delivery systems have been explored.

With that purpose, carrier-mediated delivery of curcumin has emerged as a strategic approach. Research has been carried out to find efficient drug delivery systems able to enhance

✉ Jaehong Key
jkey@yonsei.ac.kr

✉ Matteo Fasano
matteo.fasano@polito.it

[1] Department of Energy, Politecnico di Torino, Corso Duca degli Abruzzi 24, Torino 10129, Italy

[2] Department of Biomedical Engineering, Yonsei University, Wonju 26493, Gangwon State, Republic of Korea

Published online: 19 June 2024

the poor solubility and retention time of curcumin in aqueous media [7, 8]. Several nanocarriers have been developed over the years, following different approaches [9–13]. However, only a few of them are clinically approved [14–16]. Among them, poly(lactic-co-glycolic acid) PLGA is attracting more attention due to its biocompatibility, biodegradability, and FDA approval [17, 18]. PLGA-based microparticles are widely used for the sustained release of drugs because they have several advantages over traditional pharmaceutical dosage forms [19–22]. The mechanism of drug release is usually directly related to the diffusion, swelling, erosion, and degradation of the polymer matrix [23]. It is generally accepted that PLGA is hydrolyzed by erosion to produce water and carbon dioxide from the intermediate lactic acid and glycolic acid monomers [24]. Another property of the PLGA polymers used to tailor drug release is their ability to hydrate. Therefore, changes in polymer water uptake lead to swelling and its eventual dissolution [25].

Nowadays sophisticated computational tools are available to design and optimize efficient nano and micro drug delivery systems, which otherwise require long and expensive experimental tests [26–29]. The intrinsic nature of micro/nano diffusion systems relies on different spatial and temporal scale phenomena, thus requiring the adoption of an approach able to span from the discrete to continuum domain [30, 31]. Numerous *in silico* investigations [32–36, 74] have been carried out to study and predict properties and biomolecular behaviors of PLGA at multiple scales. Some studies in this context [37, 38] have used a design of experiment (DOE) to highlight correlations between input parameters and their outputs, providing valid conclusions with minimal experimental tests, time, and cost. As an example, Iman Salahshoori et al. [37] used a DOE coupled to molecular dynamics (MD) simulations to study the effect of silica nanoparticle loadings, temperature, and pressure on the transport properties of CO_2, CH_4, and N_2 gases in a PSF-PEG-silica mixed matrix membrane.

However, the relation between curcumin diffusion through hydrated PLGA and the physical-chemical features of this system has never been assessed with molecular precision, despite being the fundamental step of a multi-scale method to assist the development of PLGA-based drug delivery systems. In this work, we combined MD simulations with the creation of a DOE [39], and a sensitivity analysis [40] to highlight important relations between the parameters investigated — namely the length of the PLGA chain (L), the hydration level (H) of the system, and the PLGA density (P) – and the diffusion of curcumin in a representative volume element of PLGA-based drug delivery systems. In perspective, the present investigation could lead to a more rational design of curcumin release from Discoidal Polymeric Particles (DPPs) made of PLGA. Beyond the specific study case addressed here, we aim to propose a structured computational protocol to assist the design of drug release systems.

Materials and methods

Molecular dynamics simulations

The computational system was created to mimic a representative volume element of curcumin-loaded PLGA DPPs (see Fig. 1a) [41, 42]. Thus, the simulated system consisted of a curcumin molecule immersed in a box composed by PLGA chains and filled with water (see Fig. 1b). MD simulations were performed in GROMACS. The topology of poly-lactic acid (PLA) and poly-glycolic acid (PGA), as well as curcumin molecules (see Fig. 1c and d), were obtained from Protein Data Bank [43–45]. The PLA and PGA monomers were linked to create PLGA copolymer chains using the Polymer Modeler tool on nanoHUB [46]. The chains were generated with a random distribution of monomer residues. Three types of PLGA chains were examined, each with different lactic:glycolic molar ratios and varying lengths: 1.8 nm (0.40:0.60), 5.0 nm (0.46:0.54), and 14.7 nm (0.50:0.50).

The single chains were then packed to achieve a larger computational domain of bulk PLGA using the software Packmol [47]. According to the different PLGA chain lengths and densities, up to 60 chains were included in the computational domain. The CHARMM force field was considered [48], one of the most adopted force fields in biomolecular and drug design studies [49]. Moreover, the CHARMM force field is already parametrized both for curcumin and PLGA without requiring further fundamental computational iterations, such as *ab initio* or density functional theory simulations, to obtain the necessary parameters for molecular dynamics simulations. CHARMM parameters were downloaded from SwissParam [50]. Nonbonded interactions with up to 1.2 nm cut-off radius were considered, being long-range electrostatic interactions computed with the PME method [51] (10^{-4} accuracy, 0.4 nm spacing grid). The SPC/E [52] model was considered for the water molecules. The number of water molecules added to each configuration depended on the hydration level set for each simulation (see Tables S3 and S4 for information about the box size and number of water molecules in each simulation).

For the preliminary energy minimization step, the steepest descent algorithm was used. The system was then equilibrated at 300 K considering several NVT and NPT simulations (time constant for temperature and pressure coupling equal to $\tau_T = 0.2$ ps and $\tau_P = 3$ ps, respectively) to achieve the target PLGA/water density. Temperature and pressure equilibration was carried until steady state, with runs lasting 4 ns or more. Finally, the production run was carried out

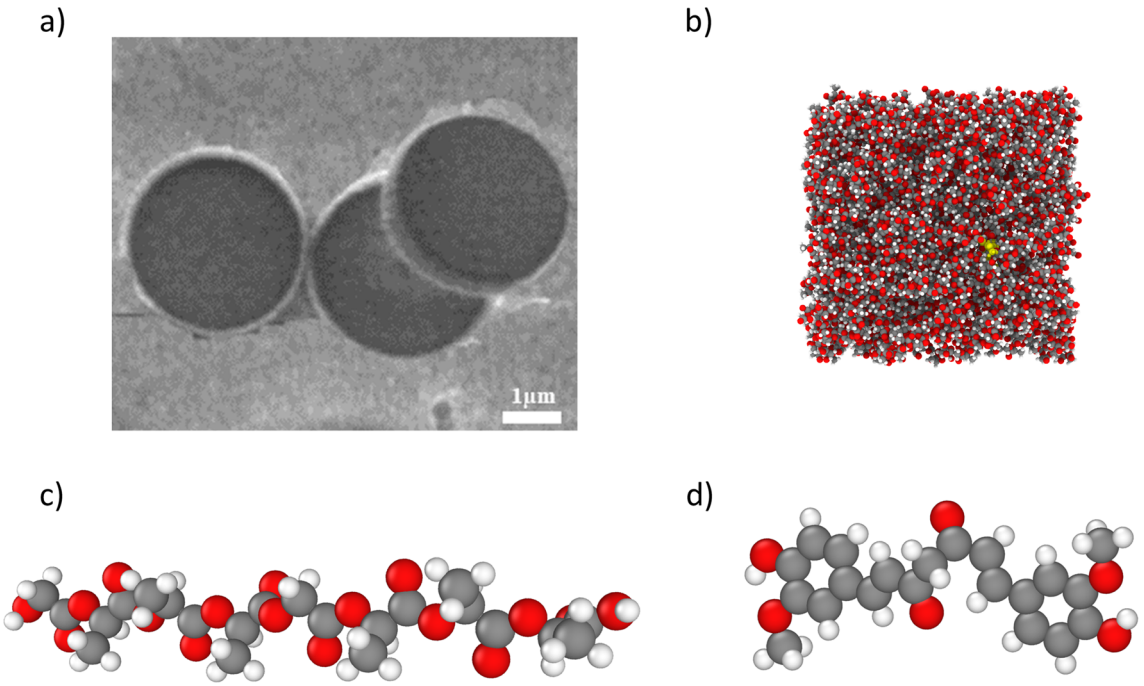

Fig. 1 **a** Morphology of curcumin-loaded DPPs using Scanning Electron Microscope; **b** rendering of a simulated PLGA box, filled with curcumin (in yellow) and water; **c** rendering of a single chain of PLGA; **d** rendering of a single molecule of curcumin. Colors in **c** and **d** indicate different atoms type: carbon in grey, oxygen in red, and hydrogen in white

considering an NVT ensemble with Nosè-Hoover thermal coupling. This thermostat (target temperature: 300 K; time constant coupling: 0.2 ps) was applied to the three groups of atoms that build up the system (water, PLGA, curcumin) to avoid any hot solvent-cold solute issue [53]. Production runs lasted 5 ns to have enough statistics to extrapolate results.

The isotropic diffusion coefficient D was evaluated considering the mean square displacement (MSD) of individual atoms of each species in the system as a function of the observation time using the classical Einstein relation for Brownian motion [54]:

$$MSD = \lim_{t\to\infty} <\| \vec{x_i}(t) - \vec{x_i}(0) \|^2>= 6Dt. \quad (1)$$

MSD data were computed along trajectories of 5 ns for each species of the system (see, for instance, Fig. 2a, b, and c). A linear fit was performed on the MSD over time. For each simulation, a linear region was identified (see Supplementary Figs. S1-S6 for MSD and Tables S1-S2 for the linear fitting time intervals considered for all configurations), and diffusion coefficients were derived from these linear sections. Additionally, a test simulation from DOE1 was extended to 10 ns to check system convergence and autocorrelation: the percentage relative errors between the 10 ns and 5 ns simulations were then computed for each species, yielding a limited discrepancy of 4.82% for water, 2.14% for curcumin, and 0.42% for PLGA in terms of D values (see Supplementary Fig. S7). The Tukey's fences inspection [55] was adopted

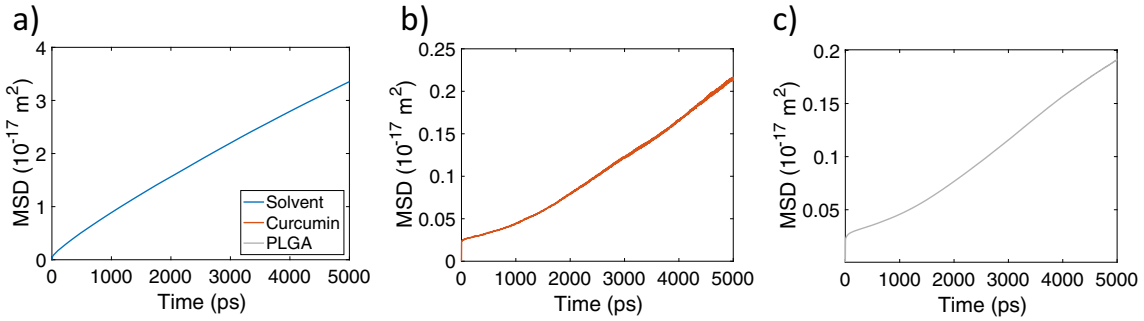

Fig. 2 Exemplified mean square displacement (MSD) of **a** solvent, **b** curcumin, and **c** PLGA

to eliminate possible outliers among the acquired data (see Supplementary Note 1).

Design of experiment

A design of experiment (DOE) approach was followed to gain deeper insights and correlations between the input parameters and the corresponding outputs of the simulations. A combination of sensitivity analysis (SA) with the DOE technique generally helps to obtain the most reliable results in this context. The chosen structure of the DOE was the Taguchi method [56], which is a simplified alternative to a full-factorial method (FFM) [57]. More information regarding the Taguchi method and how it was adopted in these MD simulations can be found in Supplementary Note 2. The input parameters selected for the DOE included hydration level (H), PLGA chain length (L), and PLGA density (P).

In a first set of numerical experiments (DOE1), three different levels were considered for each parameter, namely: L =1.8 nm, 5.0 nm, and 14.7 nm; H =0.600 g/cm^3, 0.800 g/cm^3, and 1.000 g/cm^3; P =0.804 g/cm^3, 1.072 g/cm^3, and 1.340 g/cm^3. Notice that the upper bound of L was determined on the basis of the maximum box size that could be simulated with the available computational facilities; the highest value of H was the bulk density of water at the simulated thermodynamic conditions, meaning capillary condensation and thus full hydration of the PLGA carrier; the upper bound of P was considered as the bulk density value of PLGA — lower values could be possibly achieved when swelling occurs. Hence, the L9 Taguchi orthogonal matrix was designed, providing the 9 configurations to be simulated (see Table 1). To better investigate the behavior of the system in a broader range of hydration levels — which showed to be an important factor determining D — a second set of experiments (DOE2) was performed, considering the same parameter levels of DOE1 but H = 0.000 g/cm^3, 0.300 g/cm^3, and 0.600 g/cm^3 (see Table 2).

Table 1 Taguchi orthogonal matrix for the DOE1, where L indicates the PLGA chain length, H the hydration level, and P the PLGA density

	L (nm)	H (g/cm^3)	P (g/cm^3)
1	1.8	0.6	0.804
2	1.8	0.8	1.072
3	1.8	1.0	1.340
4	5.0	0.6	1.072
5	5.0	0.8	1.340
6	5.0	1.0	0.804
7	14.7	0.6	1.340
8	14.7	0.8	0.804
9	14.7	1.0	1.072

Table 2 Taguchi orthogonal matrix for the DOE2, where L indicates the PLGA chain length, H the hydration level, and P the PLGA density

	L (nm)	H (g/cm^3)	P (g/cm^3)
1	1.8	0.0	0.804
2	1.8	0.3	0.804
3	5.0	0.0	1.072
4	5.0	0.3	1.072
5	5.0	0.6	1.072
6	14.7	0.0	1.340
7	14.7	0.3	1.340
8	14.7	0.6	1.340
(9)	1.8	0.6	0.804

Notice that the configuration 9 of DOE2 is the same than the configuration 1 of DOE1

After calculating the D of water, PLGA, and curcumin from MD simulations, the response space could be determined. The goal was to find a correlation representing the response trends across the range of design variables. A multiple linear regression model was initially considered for fitting MD results:

$$\ln(D) = C + A_1 \cdot L + A_2 \cdot H + A_3 \cdot P, \tag{2}$$

being A_i and C fitting coefficients. A logarithmic transformation was adopted for D in Eq. 2, given the various orders of magnitude explored by the different diffusion mechanisms. Subsequently, a more sophisticated multiple linear regression model with interaction terms was explored in the form of:

$$\begin{aligned}\ln(D) = {} & C + A_1 \cdot L + A_2 \cdot H + A_3 \cdot P \\ & + B_1 \cdot L \cdot H + B_2 \cdot P \cdot L + B_3 \cdot P \cdot H,\end{aligned} \tag{3}$$

being A_i, B_i, and C fitting coefficients. Notice that the regression analysis was performed considering the following measurement units: $[D]$ = μm^2/s, $[L]$ = nm, $[H]$ = g/cm^3, and $[P]$ = g/cm^3. To avoid over-fitting, no further increase in the model degree was considered.

Results and discussion

Molecular dynamics results

As a reference, we initially tested a single curcumin in a water box (cubic domain with 10 nm side; T = 300 K and p = 1 bar) observing $D = 1.0 \times 10^{-10}$ m^2/s for the curcumin, showing a box size-independent value. This result is in the same order of magnitude of previous data in the literature: for instance, Ilnytskyi et al. [58] reported $D = 4.0 \times 10^{-10}$

m^2/s for a single curcumin molecule in water, being the difference ascribable to the smaller computational domain and the coarser OPLS-UA (united atoms) force-field employed in this previous work.

In Fig. 3, we present the calculated diffusion coefficients for both DOE1 and DOE2 configurations in logarithmic scale, categorized by the three species present in the system (see Supplementary Tables S1 and S2 for tabulated results). The reported D values were calculated from stable MSD (see Supplementary Note 3 and Supplementary Figs. S1, S2, S3, S4, S5, and S6), thus assuring steady-state measures. In general, as observed in both DOE1 and DOE2, the diffusivity of water is higher than that of the other two materials (see Fig. 3a and d), due to its lower molecular weight [59, 60]. The average self-diffusion coefficient of water in the different configurations tested is found to be $D = 5.2 \times 10^{-11}$ m^2/s, being sensibly lower than its bulk value at ambient conditions ($2.4 - 2.7 \times 10^{-9}$ m^2/s [61]). This evidence demonstrates a nanoconfined state of water and thus reduced mobility, coherently with previous observations in the literature [62–67]. As evident in Fig. 3a and d, the degree of water nanoconfinement and thus D value is strongly related with the tested configuration, with different sensitivities with respect to L, H, and P parameters.

Results in Fig. 3c and f show that the D of curcumin through the hydrated PLGA is significantly lower as compared with that of curcumin in water alone, because of the enhanced diffusion resistance induced by PLGA chains. The obtained curcumin diffusion coefficients lie in a range between $D = 2.2 \times 10^{-14}$ m^2/s (configuration 5, DOE1) and 9.4×10^{-12} m^2/s (configuration 2, DOE2), obtaining comparable values with respect to previous results in the literature analyzing similar — but not identical — setups [58, 68–70]. In detail, Samanta and Roccatano [68] performed MD simulations of curcumin and pluronic block copolymer in different liquid environments, observing a value of diffusion coefficient of curcumin as low as $D = 6.0 \times 10^{-11}$ m^2/s. This value is slightly higher than our obtained interval, likely due to the fact that the system and the boundary conditions simulated are different. Karataş et al. [69] carried out density functional theory (DFT) and MD simulations of curcumin and PLGA, obtaining curcumin diffusion values up to 4.6×10^{-13} m^2/s depending on the simulated configuration. This value lies in our range, confirming the routine adopted and the reliability of the results obtained. Furthermore, Burin and colleagues [70] showed effective diffusion coefficients of molecules — with comparable molecular weight with respect to curcumin — through PLGA in the order of 10^{-13} m^2/s.

Comparing the diffusion coefficients of curcumin and PLGA in Fig. 3b, c, e, and f, a similar pattern and thus sensitivity can be noticed with respect to L, H, and P parameters. The comparable D values for both curcumin and PLGA are due to their similar molecular weight, at least for the relatively short PLGA chains simulated here. Furthermore, higher

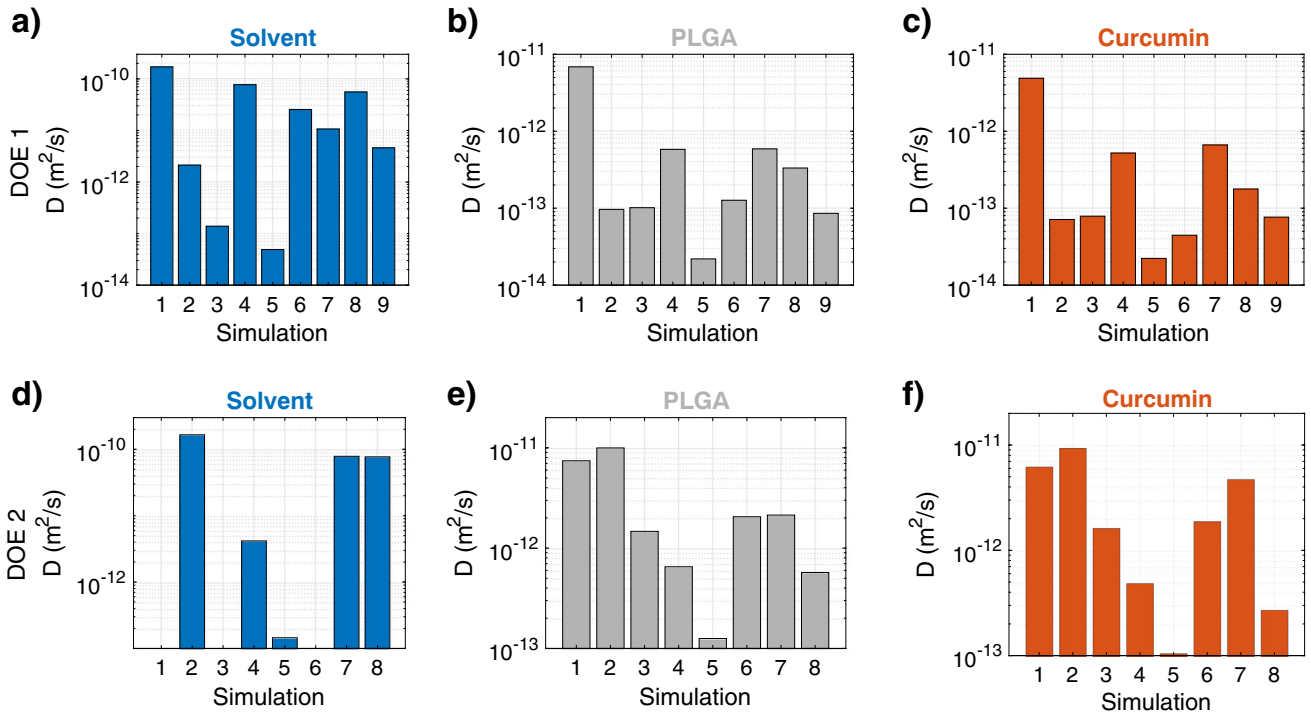

Fig. 3 Histograms of diffusion coefficient (D) for water (**a** and **d**), PLGA (**b** and **e**), and curcumin (**c** and **f**) for DOE1 and DOE2, respectively — logarithmic scale

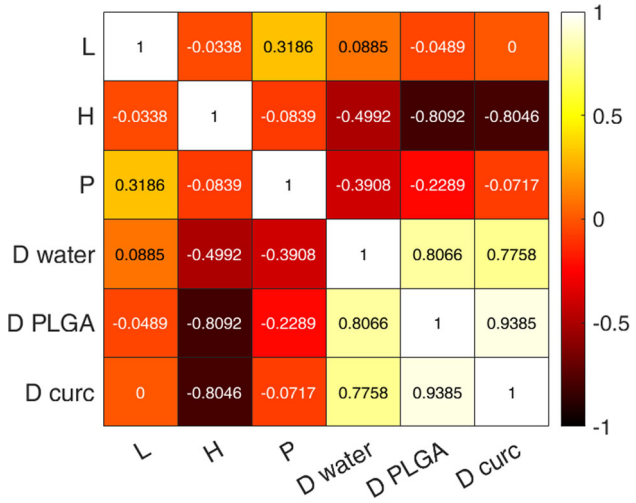

Fig. 4 Spearman's correlation coefficient (from -1 to +1, see color bar) between the input variables (hydration level H, PLGA chain length L, and PLGA density P) and the diffusion coefficients of water, PLGA, and curcumin molecules measured by MD. Levels with $H = 0$ g/cm^3 are not considered in this analysis, to avoid null values of water diffusivity

PLGA and curcumin diffusivities are generally noticed in configurations with lower water nanoconfinement (i.e., higher D in Fig. 3a and d), being water viscosity lower in such conditions [71]. Interestingly, the diffusivity of both curcumin and PLGA measured in the DOE1 show a limited variability of values around $D \sim 10^{-13}$ m^2/s for the different combinations of L, H, and P parameters except for configuration 1, which presents higher $D \sim 10^{-11}$ m^2/s instead (see Fig. 3b and c). This can be attributed to the fact that the configuration 1 has the lowest level of hydration, PLGA density, and length among the considered computational domains of DOE1, which all lead to a reduced steric occupation and thus diffusion resistance for the curcumin and PLGA motion. Such evidence is corroborated by the higher diffusivities of curcumin in the order of $D \sim 10^{-12}$ m^2/s more frequently observed in the DOE2, where lower hydration levels are explored. Therefore, an inverse correlation between D and H can be clearly noticed, while more quantitative regression analyses are required to disentangle the effects of L and P on diffusivity as well.

Such qualitative correlation evidence is systematically analyzed by computing the Spearman's correlation coefficient between the considered input variables and the obtained diffusivities (see Fig. 4). The analysis confirms a strong positive correlation between the diffusion coefficients of PLGA and curcumin but also highlights their positive correlation with water self-diffusivity. In contrast, H is shown to be strongly inversely correlated with the diffusivity of curcumin and PLGA, while a milder correlation is observed with that of water. A more moderate inverse correlation is also visible between P and the molecule's diffusivities, while L appears to have a negligible impact on them.

Regression and sensitivity analysis

A regression was then carried out on the complete set of MD results, considering both DOE1 and DOE2, to understand the sensitivity of each input parameters (L, H, and P) on the diffusion coefficient of curcumin (D_c from now on), which is the key parameter to design drug delivery systems made of PLGA. Considering Eq. 2 as fitting model, the best regression ($R^2_{adj} = 0.70$) is achieved with:

$$\ln(D_c) = 4.957 - 0.001 \cdot L - 4.363 \cdot H - 3.075 \cdot P. \quad (4)$$

To visualize Eq. 4 in the range of input parameters explored in this work, a 2D color map is reported in Fig. 5, where each dot represents one of the simulated configurations. In the first two panels, where the PLGA length is kept fixed to the minimum (Fig. 5a) and to the maximum (Fig. 5b) value tested, we observe diagonal contour plots, revealing a comparable influence of PLGA density and hydration level on D_c. Moreover, the difference between Fig. 5a and b is minimal, thus indicating the marginal role of PLGA length — at least in the considered range. On the other hand, going from the minimum (Fig. 5c) to the maximum (Fig. 5d) value of PLGA density, the color distribution changes significantly, demonstrating a key role of PLGA density in determining D_c. Additionally, as previously noted, lower hydration levels lead to increasing diffusion coefficients; whereas, no significant changes of D_c with PLGA length are evident again.

To better quantify and compare the sensitivity of D_c with the different input parameters, standardized regression coefficients were computed as [72]:

$$A_{i,STD} = A_i \frac{S_{X_i}}{S_Y}, \quad (5)$$

where A_i are the best-fitted regression coefficients in Eq. 4, S_{X_i} the standard deviations of the related input data, and S_Y the standard deviation of the output. The standardized regression coefficients delineate the extent to which a dependent variable changes for each increase in the standard deviation of the independent variable.

In our case, we found that the standardized coefficient of PLGA length is -0.004, while for hydration level is -0.787, and finally for PLGA density is -0.357. This means that the hydration level and PLGA density hold the most substantial influence on D_c through an inverse proportionality, whereas the impact of the PLGA length can be considered negligible in comparison to the other two parameters. In detail, the negative values of the standardized coefficients in the linear fit equation for H and L corroborate that — at a given box size — an increasing number of water and PLGA molecules is related to higher steric hindrance and reduced free volume available for curcumin diffusion. We

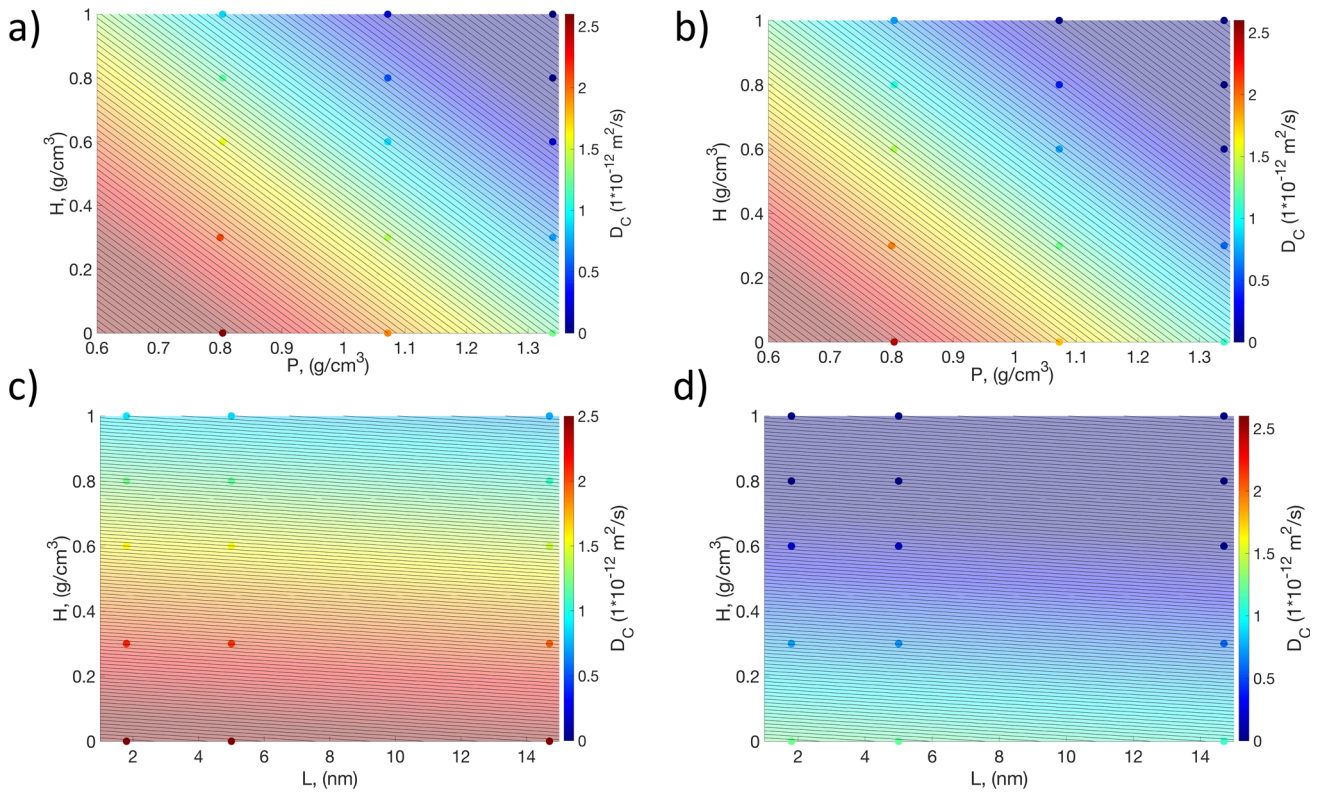

Fig. 5 Diffusion coefficient of curcumin (D_c) as a function of the hydration level (H), PLGA chain length (L), and PLGA density (P) explored by MD in this study (dots), and best fitted by Eq. 4 (background, continuous color). **a** $L = 1.8$ nm. **b** $L = 14.7$ nm. **c** $P = 0.804$ g/cm^3. **d** $P = 1.340$ g/cm^3

remark that the simulated range of L was limited by the computational feasibility of the simulated domain; however, the longer chains typically available experimentally could also lead to increased entanglement and slower mobility of the polymer matrix, consequently causing a different sensibility of D_c on L, which should therefore investigated further via, e.g., mesoscopic simulations.

Finally, the linear regression model with interaction terms in Eq. 3 was best fitted to obtain an improved prediction accuracy ($R^2_{adj} = 0.78$), that is:

$$\ln(D_c) = 8.205 - 0.422 \cdot L - 6.014 \cdot H - 6.447 \cdot P \quad (6)$$
$$-0.01 \cdot L \cdot H + 0.410 \cdot P \cdot L + 1.918 \cdot P \cdot H.$$

The enhanced interpolation of MD results for D_c can be appreciated also in Fig. 6, where the computed values from numerical simulations are compared with the predicted values from Eq. 6. In perspective, Eq. 6 could be adopted to

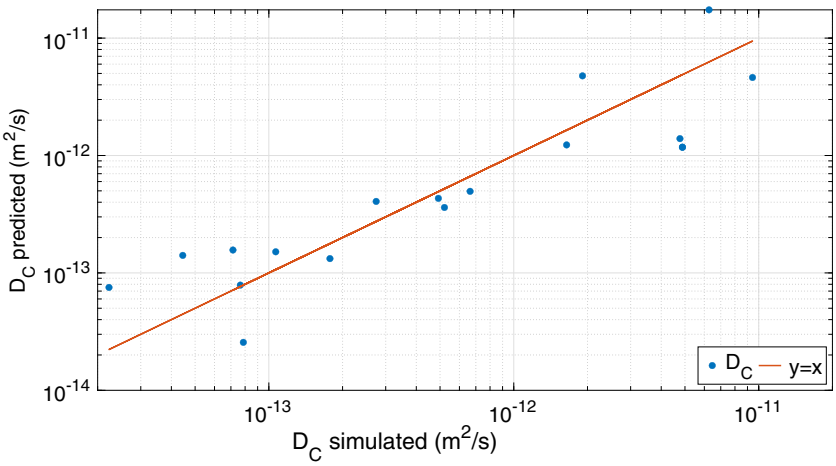

Fig. 6 Comparison between the diffusion coefficient of curcumin (D_c) calculated with MD simulations and predicted by regression Eq. 6. Points lying on the identity line correspond to the highest regression accuracy

link molecular simulations with continuum approaches in multi-scale models of curcumin diffusion and release from PLGA-based carriers, where further effects like advection, thermophoresis, particle swelling, or degradation should be considered as well.

Conclusions

Nano- and micro-technology can be a powerful tool for synthesizing and improving drug delivery systems, targeting specific sites in the body without damaging healthy tissues and cells. Additionally, tailored drug delivery systems help to release and monitor the drug dose over a specific time interval, becoming independent of cumbersome machinery and medical routines that debilitate daily activities [73]. Nevertheless, there is a lack of understanding that can link the drug diffusion process to the design parameters of the delivery system. For this reason, it is urgent to investigate and quantify the diffusion processes that physically govern the release of drugs from carriers with molecular precision. The use of PLGA as the carrier is among the most studied and promising materials for drug delivery systems, thanks to its superior biodegradability and biocompatibility characteristics. On the other hand, curcumin has promising anti-inflammatory, and anticancer properties. Here, an *in silico* study investigated a drug delivery system composed of curcumin encapsulated in a hydrated PLGA matrix at the molecular scale.

First, the topology of the representative volume element of the system was built, considering PLGA, curcumin, and water molecules as building blocks. Afterward, molecular dynamics simulations were performed to calculate the MSD of the species at a steady state. These results were found to be stable over time, hence the diffusion coefficients were extracted using the Einstein formula for Brownian motion. The latter were found to agree with the few data found in the literature, confirming the goodness of the chosen models and the adopted routine for the simulation.

MD results showed that curcumin and PLGA have comparable values of diffusion coefficients for the considered case studies, while water has higher diffusivity due to its lighter molecular weight. The sensitivity analysis showed that the hydration level and PLGA density play the most significant role in influencing the diffusion mechanism of curcumin, while the length of the PLGA chain is negligible compared to the other two — at least for the simulated range of values. Additionally, the coefficients of hydration level and PLGA density in the linear regression equation indicate that an increase in any of these two input parameters corresponds to a decrease in the diffusion coefficient of curcumin, this being due to the steric hindrance to curcumin diffusion. In summary, this computational approach has revealed interesting relationships between the considered input parameters and the diffusion coefficient, providing an accurate regression model to quantify them.

Overall this work represents the first step of a bottom-up multi-scale approach proposing a rational design process to assist the development of drug delivery systems such as Discoidal Polymeric Particles. Predicting the diffusion processes of drug nanoparticles into the carrier PLGA matrix depending on different material parameters and molecular configurations is a key aspect to help in the development of drug delivery particles with targeted properties. Finally, we believe that this approach can be efficiently adopted for future studies and seamlessly integrated with approaches at larger scales (e.g., finite element method).

Supplementary Information The online version contains supplementary material available at https://doi.org/10.1007/s00894-024-06023-x.

Acknowledgements The authors thank the Politecnico di Torino's High-Performance Computing Initiative (http://hpc.polito.it/) for computing resources. We acknowledge the CINECA award under the ISCRA initiative, for the availability of high performance computing resources and support.

Author Contributions M.F. and J.K. conceptualized and supervised the research. A.D.G., S.P., A.L., and E.S. carried out simulations. F.M.B. and M.F. supervised the modeling activities and interpreted the results. A.D.G., S.A., and S.P. performed validation analyses and wrote the first draft of the manuscript. All authors reviewed the final version of the manuscript.

Funding Open access funding provided by Politecnico di Torino within the CRUI-CARE Agreement. Partial financial support was received from the Italian Embassy in South Korea for traveling.

Data Availability All data generated or analyzed during this study are included in this published article and the supplementary material file.

Declarations

Ethics approval and consent to participate Not applicable

Conflict of interest The authors declare no competing interests.

References

1. Chainani-Wu N (2003) Safety and anti-inflammatory activity of curcumin: a component of tumeric (curcuma longa). The J Alter Complement Med 9(1):161–168
2. Sethiya A, Agarwal DK, Agarwal S (2020) Current trends in drug delivery system of curcumin and its therapeutic applications. Mini Rev Med Chem 20(13):1190–1232
3. Yavarpour-Bali H, Ghasemi-Kasman M, Pirzadeh M (2019) Curcumin-loaded nanoparticles: a novel therapeutic strategy in treatment of central nervous system disorders. Int J Nanomed 4449–4460
4. Shanmugam MK, Rane G, Kanchi MM, Arfuso F, Chinnathambi A, Zayed M, Alharbi SA, Tan BK, Kumar AP, Sethi G (2015) The multifaceted role of curcumin in cancer prevention and treatment. Mol 20(2):2728–2769
5. Yallapu MM, Khan S, Maher DM, Ebeling MC, Sundram V, Chauhan N, Ganju A, Balakrishna S, Gupta BK, Zafar N et al (2014) Anti-cancer activity of curcumin loaded nanoparticles in prostate cancer. Biomaterials 35(30):8635–8648
6. Anand P, Kunnumakkara AB, Newman RA, Aggarwal BB (2007) Bioavailability of curcumin: problems and promises. Mol Pharma 4(6):807–818
7. Ratrey P, Dalvi SV, Mishra A (2020) Enhancing aqueous solubility and antibacterial activity of curcumin by complexing with cell-penetrating octaarginine. ACS Omega 5(30):19004–19013
8. Mohanty C, Sahoo SK (2010) The in vitro stability and in vivo pharmacokinetics of curcumin prepared as an aqueous nanoparticulate formulation. Biomater 31(25):6597–6611
9. Din FU, Aman W, Ullah I, Qureshi OS, Mustapha O, Shafique S, Zeb A (2017) Effective use of nanocarriers as drug delivery systems for the treatment of selected tumors. Int J Nanomed 7291–7309
10. Mazdaei M, Asare-Addo K (2022) A mini-review of nanocarriers in drug delivery systems. British J Pharma 7(1):1–13
11. Amoabediny G, Haghiralsadat F, Naderinezhad S, Helder MN, Akhoundi Kharanaghi E, Mohammadnejad Arough J, Zandieh-Doulabi B (2018) Overview of preparation methods of polymeric and lipid-based (niosome, solid lipid, liposome) nanoparticles: a comprehensive review. Int J Pol Mater Pol Biomater 67(6):383–400
12. Key J, Palange AL, Gentile F, Aryal S, Stigliano C, Di Mascolo D, De Rosa E, Cho M, Lee Y, Singh J et al (2015) Soft discoidal polymeric nanoconstructs resist macrophage uptake and enhance vascular targeting in tumors. ACS Nano 9(12):11628–11641
13. Di Mascolo D, Palange AL, Primavera R, Macchi F, Catelani T, Piccardi F, Spanò R, Ferreira M, Marotta R, Armirotti A et al (2021) Conformable hierarchically engineered polymeric micromeshes enabling combinatorial therapies in brain tumours. Nat Nanotechnol 16(7):820–829
14. Barenholz YC (2012) Doxil®-the first FDA-approved nano-drug: lessons learned. J Control Release 160(2):117–134
15. Namiot ED, Sokolov AV, Chubarev VN, Tarasov VV, Schiöth HB (2023) Nanoparticles in clinical trials: analysis of clinical trials, FDA approvals and use for COVID-19 vaccines. Int J Mol Sci 24(1):787
16. Bobo D, Robinson KJ, Islam J, Thurecht KJ, Corrie SR (2016) Nanoparticle-based medicines: a review of FDA-approved materials and clinical trials to date. Pharma Res 33:2373–2387
17. Yallapu MM, Gupta BK, Jaggi M, Chauhan SC (2010) Fabrication of curcumin encapsulated PLGA nanoparticles for improved therapeutic effects in metastatic cancer cells. J Colloid Interface Sci 351(1):19–29
18. Ganesan M, Paranthaman S (2021) Molecular structure, interactions, and antimicrobial properties of curcumin-PLGA complexes–a DFT study. J Mol Model 27:1–12
19. Bao T-Q, Hiep N-T, Kim Y-H, Yang H-M, Lee B-T (2011) Fabrication and characterization of porous poly (lactic-co-glycolic acid)(PLGA) microspheres for use as a drug delivery system. J Mater Sci 46:2510–2517
20. Nguyen TTT, Ghosh C, Hwang S-G, Tran LD, Park JS (2013) Characteristics of curcumin-loaded poly (lactic acid) nanofibers for wound healing. J Mater Sci 48:7125–7133
21. Chelopo MP, Kalombo L, Wesley-Smith J, Grobler A, Hayeshi R (2017) The fabrication and characterization of a PLGA nanoparticle-pheroid® combined drug delivery system. J Mater Sci 52:3133–3145
22. Jiang L, Ma Y, Tang S, Zhang Y, Su S (2023) Poly (lactide-co-glycolide)-based nanocomposite reinforced by a novel hybrid nanohydroxyapatite. J Mater Sci 58(44):16954–16971
23. Hines DJ, Kaplan DL (2013) Poly (lactic-co-glycolic) acid-controlled-release systems: experimental and modeling insights. Crit Rev^{TM} Ther Drug Carrier Syst 30(3)
24. Jain GK, Pathan SA, Akhter S, Ahmad N, Jain N, Talegaonkar S, Khar RK, Ahmad FJ (2010) Mechanistic study of hydrolytic erosion and drug release behaviour of PLGA nanoparticles: influence of chitosan. Polym Degrad Stab 95(12):2360–2366
25. D'Souza S, Dorati R, DeLuca PP (2014) Effect of hydration on physicochemical properties of end-capped plga. Adv Biomater 2014
26. Decuzzi P (2016) Facilitating the clinical integration of nanomedicines: the roles of theoretical and computational scientists. ACS Nano 10(9):8133–8138
27. Gizzatov A, Key J, Aryal S, Ananta J, Cervadoro A, Palange AL, Fasano M, Stigliano C, Zhong M, Di Mascolo D et al (2014) Hierarchically structured magnetic nanoconstructs with enhanced relaxivity and cooperative tumor accumulation. Adv Func Mater 24(29):4584–4594
28. Bergamasco L, Morciano M, Fasano M (2021) Effect of water nanoconfinement on the dynamic properties of paramagnetic colloidal complexes. Phys Chem Chem Phys 23(31):16948–16957
29. Bergamasco L, Alberghini M, Fasano M (2019) Nano-metering of solvated biomolecules or nanoparticles from water self-diffusivity in bio-inspired nanopores. Nanoscale Res Lett 14:1–11
30. Cardellini A, Fasano M, Chiavazzo E, Asinari P (2015) Mass transport phenomena at the solid-liquid nanoscale interface in biomedical application. In: COUPLED VI: Proceedings of the VI International Conference on Computational Methods for Coupled Problems in Science and Engineering. CIMNE , pp 593–604
31. Fasano M, Borri D, Cardellini A, Alberghini M, Morciano M, Chiavazzo E, Asinari P (2017) Multiscale simulation approach to heat and mass transfer properties of nanostructured materials for sorption heat storage. Energy Procedia 126:509–516
32. Stipa P, Marano S, Galeazzi R, Minnelli C, Mobbili G, Laudadio E (2021) Prediction of drug-carrier interactions of PLA and PLGA drug-loaded nanoparticles by molecular dynamics simulations. Eur Polymer J 147:110292
33. Megy S, Aguero S, Da Costa D, Lamrayah M, Berthet M, Primard C, Verrier B, Terreux R (2020) Molecular dynamics studies of poly (lactic acid) nanoparticles and their interactions with vitamin e and tlr agonists pam1csk4 and pam3csk4. Nanomater 10(11):2209
34. Pannuzzo M, Horta BA, La Rosa C, Decuzzi P (2020) Predicting the miscibility and rigidity of poly (lactic-co-glycolic acid)/polyethylene glycol blends via molecular dynamics simulations. Macromol 53(10):3643–3654
35. Asadzadeh H, Moosavi A (2019) Investigation of the interactions between melittin and the PLGA and PLA polymers: molecular dynamic simulation and binding free energy calculation. Materials Research Express 6(5):055318
36. Andrews J, Handler RA, Blaisten-Barojas E (2020) Structure, energetics and thermodynamics of PLGA condensed phases from molecular dynamics. Polymer 206:122903

37. Chagarov E, Adams JB, Kieffer J (2004) Application of design of experiments methodology to optimization of classical molecular dynamics generation of amorphous sio2 structure. Modell Simul Mater Sci Eng 12(2):337
38. Gupta R, Xie H, Sarkar M, Chen Y (2022) Design of experiment (doe) for optimization of PLGA nanoparticles. The FASEB J 36
39. Jankovic A, Chaudhary G, Goia F (2021) Designing the design of experiments (doe)-an investigation on the influence of different factorial designs on the characterization of complex systems. Energy Build 250:111298
40. Mowbray FI, Manlongat D, Shukla M (2022) Sensitivity analysis: a method to promote certainty and transparency in nursing and health research. Canadian J Nurs Res 54(4):371–376
41. Nishu SD, Park S, Ji Y, Han I, Key J, Lee TK (2020) The effect of engineered PLGA nanoparticles on nitrifying bacteria in the soil environment. J Ind Eng Chem 84:297–304
42. Choi S, Lee S-H, Park S, Park SH, Park C, Key J (2021) Indocyanine green-loaded PLGA nanoparticles conjugated with hyaluronic acid improve target specificity in cervical cancer tumors. Yonsei Med J 62(11):1042
43. Zardecki C, Dutta S, Goodsell DS, Lowe R, Voigt M, Burley SK (2022) Pdb-101: educational resources supporting molecular explorations through biology and medicine. Protein Sci 31(1):129–140
44. Lactic acid structure - RCSB Protein Data Bank (2022) https://web.archive.org/web/20240513144441/https://www.rcsb.org/ligand/LAC
45. Glycolic acid structure - RCSB Protein Data Bank (2022) https://web.archive.org/web/20240513144314/https://www.rcsb.org/ligand/GOA
46. Madhavan K, Zentner L, Farnsworth V, Shivarajapura S, Zentner M, Denny N, Klimeck G (2013) Nanohub. org: cloud-based services for nanoscale modeling, simulation, and education. Nanotechnol Rev 2(1):107–117
47. Martínez L, Andrade R, Birgin EG, Martínez JM (2009) Packmol: a package for building initial configurations for molecular dynamics simulations. J Comput Chem 30(13):2157–2164
48. Bjelkmar P, Larsson P, Cuendet MA, Hess B, Lindahl E (2010) Implementation of the charmm force field in gromacs: analysis of protein stability effects from correction maps, virtual interaction sites, and water models. J Chem Theory Comput 6(2):459–466
49. Vanommeslaeghe K, MacKerell Jr A (2015) Charmm additive and polarizable force fields for biophysics and computer-aided drug design. Biochimica et Biophysica Acta (BBA)-General Subjects 1850(5):861–871
50. Zoete V, Cuendet MA, Grosdidier A, Michielin O (2011) Swissparam: a fast force field generation tool for small organic molecules. J Comput Chem 32(11):2359–2368
51. Petersen HG (1995) Accuracy and efficiency of the particle mesh Ewald method. J Chem Phys 103(9):3668–3679
52. Berendsen HJ, Grigera JR, Straatsma TP (1987) The missing term in effective pair potentials. J Phys Chem 91(24):6269–6271
53. Fuzo CA, Degrève L (2012) Effect of the thermostat in the molecular dynamics simulation on the folding of the model protein chignolin. J Mol Model 18:2785–2794
54. Hansen J-P, McDonald IR (2013) Theory of simple liquids: with applications to soft matter. Academic press, Cambridge (USA)
55. Barnett V (1983) Principles and methods for handling outliers in data sets. In: Statistical Methods and the Improvement of Data Quality. Elsevier, pp 131–166
56. Karna SK, Sahai R et al (2012) An overview on Taguchi method. Int J Eng Math Sci 1(1):1–7
57. Antony J (2023) Design of experiments for engineers and scientists. Elsevier
58. Ilnytskyi J, Patsahan T, Pizio O (2016) On the properties of the curcumin molecule in water. Exploration of the opls-united atom model by molecular dynamics computer simulation. J Mol Liquids 223:707–715
59. Kuo I-FW, Mundy CJ, McGrath MJ, Siepmann JI, VandeVondele J, Sprik M, Hutter J, Chen B, Klein ML, Mohamed F et al (2004) Liquid water from first principles: investigation of different sampling approaches. J Phys Chem B 108(34):12990–12998
60. Gallo P, Amann-Winkel K, Angell CA, Anisimov MA, Caupin F, Chakravarty C, Lascaris E, Loerting T, Panagiotopoulos AZ, Russo J et al (2016) Water: a tale of two liquids. Chem Rev 116(13):7463–7500
61. Bellussi FM, Roscioni OM, Ricci M, Fasano M (2021) Anisotropic electrostatic interactions in coarse-grained water models to enhance the accuracy and speed-up factor of mesoscopic simulations. J Phys Chem B 125(43):12020–12027
62. Chiavazzo E, Fasano M, Asinari P, Decuzzi P (2014) Scaling behaviour for the water transport in nanoconfined geometries. Nat Commun 5(1):1–11
63. Cardellini A, Fasano M, Chiavazzo E, Asinari P (2016) Interfacial water thickness at inorganic nanoconstructs and biomolecules: size matters. Phys Lett A 380(20):1735–1740
64. Camargo D, La Torre J, Duque-Zumajo D, Español P, Delgado-Buscalioni R, Chejne F (2018) Nanoscale hydrodynamics near solids. The J Chem Phys 148(6)
65. Fasano M, Bevilacqua A, Chiavazzo E, Humplik T, Asinari P (2019) Mechanistic correlation between water infiltration and framework hydrophilicity in mfi zeolites. Sci Rep 9(1):18429
66. Leverant CJ, Harvey JA, Alam TM, Greathouse JA (2021) Machine learning self-diffusion prediction for Lennard-Jones fluids in pores. The J Phys Chem C 125(46):25898–25906
67. Casto A, Bellussi FM, Diego M, Del Fatti N, Banfi F, Maioli P, Fasano M (2023) Water filling in carbon nanotubes with different wettability and implications on nanotube/water heat transfer via atomistic simulations. Int J Heat Mass Transf 205:123868
68. Samanta S, Roccatano D (2013) Interaction of curcumin with peoppo-peo block copolymers: a molecular dynamics study. J Phys Chem B 117(11):3250–3257
69. Karataş D, Tekin A, Bahadori F, Çelik MS (2017) Interaction of curcumin in a drug delivery system including a composite with poly (lactic-co-glycolic acid) and montmorillonite: a density functional theory and molecular dynamics study. J Mater Chem B 5(40):8070–8082
70. Burin GRM, Santos TC, Battisti MA, Campos AM, Ferreira SRS, Carciofi BAM (2022) Transport properties of hydrophilic compounds in plga microspheres. Res, Soc Dev 11(16):398111638335–398111638335
71. Morciano M, Fasano M, Nold A, Braga C, Yatsyshin P, Sibley D, Goddard BD, Chiavazzo E, Asinari P, Kalliadasis S (2017) Nonequilibrium molecular dynamics simulations of nanoconfined fluids at solid-liquid interfaces. The J Chem Phys 146(24)
72. Siegel AF (2016) Practical business statistics. Academic Press, Cambridge (USA)
73. Sun J, Yang Z, Teng L (2020) Nanotechnology and microtechnology in drug delivery systems. Dose-Response 18(2):1559325820907810
74. Bellussi FM, Roscioni OM, Rossi E, Cardellini A, Provenzano M, Persichetti L, Kudryavtseva V, Sukhorukov G, Asinari P, Sebastiani M, Fasano M (2023) Wettability of soft PLGA surfaces predicted by experimentally augmented atomistic models. MRS Bulletin 48(2):108–117